

Battery and SuperCapacitor Hybridization for a Pure Electric Three-Wheel Roadster

João P. Trovão*, Maxime R. Dubois

Department of Electrical & Computer Engineering
Université de Sherbrooke / e-TESTC / *INESC Coimbra
Sherbrooke, QC, J1K 2R1, Canada
{Joao.Trovao, Maxime.Dubois,
Alain.Desrochers}@USherbrooke.ca

Abstract—This paper presents a possible scheme to integrate a SuperCapacitor pack in a full electric, battery powered, three-wheel vehicle. The proposed hybridization is built upon a fully-active parallel topology. First, a complete model based on energetic macroscopic representation is established for power energy analysis of standard driving cycles. Thereafter, the control scheme is deduced, based on the maximum control structure approach. Finally, the energy management strategy is approached using fuzzy logic controller. To validate the proposed topology, simulation results are provided for the New European Driving Cycle and World-wide Motorcycle emissions Testing Cycle.

Keywords—Electric Vehicles; SuperCapacitors; Fully-Decoupled Topology; Maximum Control Structure; Energy Management System.

I. INTRODUCTION

Electric traction is the key to better and more sustainable transportation. Battery Electric Vehicles (EVs) are one of the most promising solutions [1][2]. For pure EVs, higher focus is placed to specific power, related to acceleration and climbing capability, but also to the life of the primary Energy Storage System (ESS). Batteries are the most suitable ESS for EVs although they are limited in terms of power/energy density and charging time. Moreover, batteries with high power/energy characteristics still have a high cost [3]. Coupling batteries with other energy sources could allow attaining better global performances [3]. Thus, the hybridization of different energy sources has been studied, combining batteries, SuperCapacitors (SCs), flywheels and/or Fuel Cells (FCs) [4, 5]. For automotive applications and at the current state of technology, the most common hybridization is the use of batteries with high specific energy and SCs (high specific power). The integration topology that allows the highest level of freedom is the fully-decoupled configuration [5]. However the control of this topology is complex and may be different, depending on the vehicle operating modes [5, 6], hence requiring a robust energy management strategy.

EVs using hybrid ESS are a multifaceted systems with different dynamics and control/management objectives. Since 2000, Energetic Macroscopic Representation (EMR) is being introduced for the organization of multi-physical models in a unified way. Moreover, the control layer could be obtained using particular inversion rules [6], providing relevant inputs for the energy management strategy. EMR has been

Marc-André Roux, Éric Ménard, Alain Desrochers

Centre de Technologies Avancées BRP - UdeS
Université de Sherbrooke
Sherbrooke, QC, J1K 0A5, Canada
{Marc-Andre.Roux, Eric.Menard}@cta-brp-udes.com

successfully used for various EVs and HEVs, from simulation to real-time control, both in experimental set-ups and prototypes [6, 7].

The objective of this paper is to develop an upgraded version of a full-battery powered three-wheel roadster, presented in Fig. 1. The primary objective is to increase the driving range with a given battery and reduce the degradation of the battery pack due to hard stresses in discharge currents. The addition of a SCs pack combined to high specific energy batteries could be a first step to answer these issues. The addition of SCs to the ESS increases its cost and overall complexity. The EMR approach will be used in the model organization and will assist in the definition of the inputs/outputs of the energy strategy. As an extension of previous works [6, 7], the energy flows between the different sources (batteries, SCs, traction system) are addressed in this paper, where a new energy management system (EMS) is proposed. The EMR approach used in this paper is a crucial point in the design of an accurate EMS, which is based on fuzzy logic controller by using this organization approach to set up the membership functions of the proposed global strategy. A complete analysis is carried out in the paper, with an assessment of drawbacks and advantages of the actively controlled SC-battery hybridized topology compared to the conventional EV. A simulation of such hybridized system will be made in order to define the power/energy requirements and present some control and energy approaches using New European Driving Cycle (NEDC) and World-wide Motorcycle emissions Testing Cycle (WMTC).



Fig. 1. CTA prototype of three-wheel roadster.

The remainder of the paper is structured as follows. The three-wheel roadster model of the hybrid powertrain is described in Section II. Section III addresses the control structure and energy strategy framework. Section IV discusses and presents the simulation results for the NEDC and WMTC driving cycles, while the concluding remarks and ongoing works are outlined in Section V.

II. THREE-WHEEL ROADSTER MODEL

The original architecture of the full electric three-wheel roadster vehicle powertrain is presented in Fig. 2. This prototype is currently used as a workbench at the *Centre de Technologies Avancées* BRP - Université de Sherbrooke (CTA) [8]. For this prototype execution, a 28 kW-96V Permanent Magnet Synchronous Motor (PMSM) was selected and is directly connected to the rear wheel.

The main characteristics of the vehicle are presented in Table I. The addition of a SCs pack is actually considered for the roadster application and is the core of this paper. The SCs and the batteries are connected to the common DC bus (rated 108 V nominal) via two DC-DC converters, used to control the two energy storage elements current flow into the DC bus so as to provide the current required by the motor inverter. The corresponding EMR configuration schematic is shown in fig. 3. Although other suitable topologies have previously been discussed in the literature, the fully-decoupled configuration has been chosen in the paper. This configuration has the ability to maintain the DC bus voltage close to its nominal value.

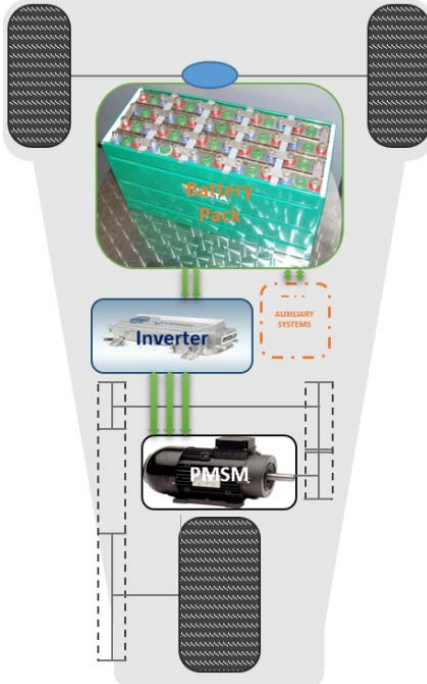


Fig. 2. Schematic of the CTA prototype original (not hybridized) powertrain.

TABLE I. ELECTRIC VEHICLE SPECIFICATIONS

Variable	Symbol	Value	Units
Vehicle mass (without bat/SC)	m	350	kg
Typical rolling resistance coefficient	μ_{rr}	0.02	-
Typical aerodynamic drag coefficient (with driver)	C_D	0.75	-
Vehicle front area	A_f	1.25	m^2
Wheels radius	r	0.305	m
Gearbox transmission ratio	G_{gb}	5.033 (30:151)	-
Gearbox transmission efficiency	η_{gb}	95	%

The prototype shown in Fig. 2 was developed at an early stage, using a DC bus determined by a Li-ion battery only. In the original EV version of the vehicle, the battery pack is directly coupled to the motor inverter, with large voltage variations, which implies large losses in the inverter and motor,

leading to temperature increases. One of the key points in the hybridized SCs-battery system with power converter on each of these sources is the ability to maintaining a constant DC bus voltage throughout the overall operation. The main Energy Storage System (ESS) with hybridized configuration has high specific energy battery pack operating at 74 V and 243 A@2C and a SCs pack with a rated voltage of 85.5 V. Their characteristics are shown in Table II.

Modeling of the mechanical and electrical components in the vehicle is necessary, as the control strategy dictating the SCs power and SoC will be determined by the vehicle mass, acceleration and speed. To that end, EMR was chosen as an instrument of model organization between mechanical and electrical components. The EMR of the powertrain system representing the different energy flows between the energy sources and the traction system is presented in Fig. 3.

EMR is a graphical description that highlights the energy properties of components within a system in order to develop control schemes [6] (see Appendix for the pictograms). Only the physical causality (i.e. integral causality) is considered. Moreover, all elements are connected according to the interaction principle: the product of the action and the reaction variables yields the power exchanged.

TABLE II. CHARACTERISTICS OF THE ENERGY STORAGE SYSTEMS

Variable	Symbol	Value	Units
Battery (3.7 V, 2.8 A, high energy LG Lithium cells)			
Battery pack Power	P_{bat}	[- 11.2, 22.4]	kW
Battery pack SoC Limits	SoC_{bat}	[0.2, 1]	-
Min. cell open-circuit voltage	$V_{bat}^{OC,min}$	3	V
cell no-load voltage drop	δ_{bat}	1.3	V
Max. cell open-circuit voltage	$V_{bat}^{OC,max}$	4.3	V
Number of cells in series	N_{bat}	20	-
Num. of cells bank in parallel	n_{bat}	45	-
Cell mass	M_{bat}	50	g
Supercapacitors (MAXWELL BC series BCAP0350 cells)			
SCs pack Capacitance	Cap_{SC}	467	F
SCs pack Power	P_{SC}	[- 330, 330]	kW
SCs pack SoC Limits	SoC_{SC}	[0.5, 1]	-
Min. SCs open-circuit voltage	$V_{SC}^{OC,min}$	0	V
SCs no-load voltage drop	δ_{SC}	2.85	V
SCs pack operation range	V_{SC}^{OC}	[42.8, 85.5]	V
Number of SCs module in series	N_{SC}	30	-
Num. of SCs bank in parallel	n_{SC}	40	-
SCs module Mass	M_{SC}	60	g

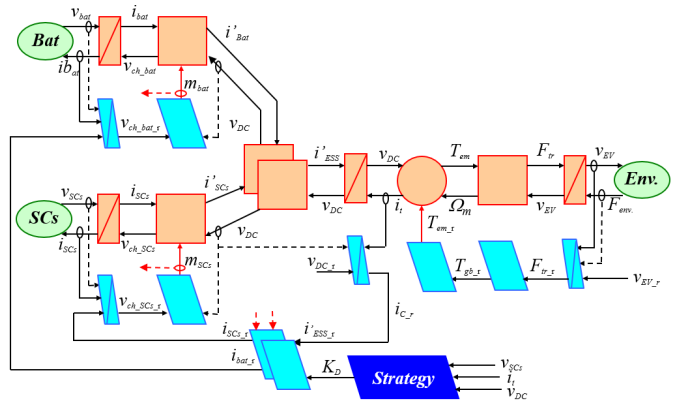


Fig. 3. EMR and Maximum Control Structure (MCS) of the powertrain.

A. Traction System Model

The mechanical action on the EV model is a source element. The action of the environment on the vehicle, modeled as a mechanical source, yields the traction force resistance F_{env} mainly composed of drag, friction and slope components, as in (1).

$$F_{env} = M_{eq} g \mu_{rr} + \frac{1}{2} \rho A_f C_d v_{EV}^2 + M_{eq} g \sin(\theta) \quad (1)$$

The chassis accumulates kinetic energy and the vehicle velocity v_{EV} is the corresponding state variable of this accumulation element, derived from the total traction force F_{tr} and the traction force resistance F_{env} :

$$M_{eq} \frac{d}{dt} v_{EV} = F_{tr} - F_{env} \quad (2)$$

where M_{eq} is the equivalent mass of the vehicle, considering the tare weight, energy sources, passengers and inertia effects.

The model of the accumulation of the kinetic energy is represented in the EMR diagram by an accumulation element. The traction force and vehicle velocity are related to the electric machine torque T_{em} and rotor rotation speed Ω_m with:

$$\begin{cases} F_{tr} = \frac{G_{gb}}{r} T_{em} \eta_{gb}^\beta \\ \Omega_m = \frac{G_{gb}}{r} v_{EV} \end{cases}, \quad \begin{cases} \beta = 1, \text{ for } P_{mec} \geq 0 \\ \beta = -1, \text{ for } P_{mec} < 0 \end{cases} \quad (3)$$

where G_{gb} is the fixed gear ratio, η_{gb} its efficiency, and r the wheel radius (see Table I). The slip phenomenon of the wheels is neglected and all inertias are merged with the vehicle mass. The integrated model of the gearbox and wheels is represented by a mono-physical conversion element.

The complete model of the traction system was developed using a generic model of the electric machine and its converter. To study the energy management problem, a static model is used [14]. This model takes into account the converter, the electric machine and its control. A reference torque (T_{em_r}) directly controls the electric machine and the current is modeled by:

$$\begin{cases} T_{em} = T_{em_r} \\ i_{load} = \frac{T_{em} \Omega_m \eta_m^\beta}{v_{DC}} \end{cases} \quad (4)$$

where η_m is the drive efficiency, including both the inverter and the PMSM. The efficiency map (see Fig. 4) is the result of the mechanical variables variation (T_{em}, Ω_m) at constant inverter voltage and constant temperature operation of the motor. The corresponding model considers the inverter, the PMSM and its control.

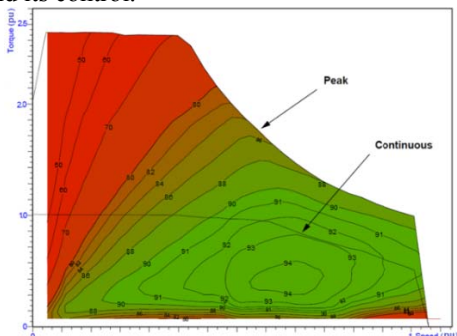


Fig. 4. Efficiency map η_m of a typical used electric drive.

B. Common DC Bus Model

The common DC bus combines two sources, the traction system and the DC bus capacitor. This capacitor, connected at the input of the Voltage Source Inverter (VSI), imposes a common voltage v_{DC} and is represented in Fig. 3 by an accumulation element (orange crossed rectangle). The capacitor voltage v_{DC} is a state variable defined from the capacitor current i_c in (5), where C is the capacitance value.

$$C \frac{dv_{DC}}{dt} = -i_c \quad (5)$$

The DC bus is represented by a distribution element (orange double square):

$$\begin{cases} i_c = i'_{ESS} - i_t \\ i_t = \sum_{j \in \{bat; SC\}} i_{ch_j} \end{cases} \quad (6)$$

C. DC-DC Converters Model

In Fig. 3, the inductors are represented as accumulation elements (orange crossed rectangles) that impose the current as a state variable (output) from different input voltages (7) with L_j and R_j being respectively the inductances and resistances of those inductors.

$$L_j \frac{d}{dt} i_j = v_j - v_{ch_j} - R_j i_j \quad j \in \{bat; SC\} \quad (7)$$

The DC-DC converters are mono-physical conversion elements (orange squares). These devices are modeled using modulation ratios m_j that connect the voltages and currents from both sides (8), where η_{Conv} is the DC-DC converter efficiency.

$$\begin{cases} v_{ch_j} = m_j v_{DC} \\ i_{ch_j} = m_j i_j \eta_{Conv}^\beta \\ m_j \in \{0, 1\} \text{ and } \begin{cases} \beta = 1, \text{ for } P_{Conv} \geq 0 \\ \beta = -1, \text{ for } P_{Conv} < 0 \end{cases} \end{cases} \quad (8)$$

D. Energy Storage Systems Model

Batteries and SCs are the energy sources (green oval pictograms). In the EMR approach, the source imposes the voltage v_j in the system, which responds with the current i_j ($j \in \{bat; SC\}$). The generic model used for the sources is defined in Fig. 5 (more details in [5]).

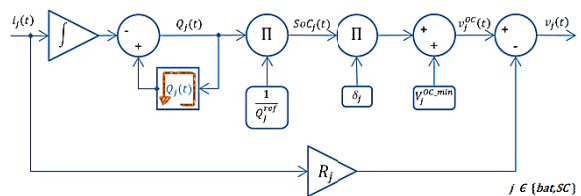


Fig. 5. Generic model adopted for ESSs.

III. CONTROL AND MANAGEMENT STRATEGY

In the three-wheel roadster application, space is critical and the use of Li-ion batteries with high specific energy is necessary. The purpose of the SCs is to provide the electrical power that the battery pack is unable to deliver in many acceleration scenarios. Bearing this principle in mind, the control of the SCs voltage and related SoC is an important issue, as emptying the SCs too quickly would be detrimental to the vehicle acceleration performance.

A Maximum Control Structure (MCS) of the EV is deduced from the EMR scheme. This MCS will be used in simulation to validate the system model. The MCS identifies the arrangement of the energy management strategy and the output type. Owing to the use of two ESS (battery and SCs) a distribution ratio is identified as a function of the total current demanded by the powertrain (see Fig. 3).

A. Maximum Control Structure (MCS)

In this control problem, two control objectives are identified. The first is the control of the DC bus voltage, v_{DC} . The second is the vehicle speed, v_{EV} . Two tuning variables, m_{SC} and m_{bat} , are used to reach the v_{DC} (Fig. 3) in the first objective, in accordance with the causality principle. The inductor currents and DC bus voltage are the state variables. For the second objective, the tuning variable T_{em_r} , is connected to v_{EV} , as presented in Fig. 3.

Following the inversion-rules of the EMR [6] the control layer is obtained. The inversion-based control scheme is composed of four controllers and a management strategy algorithm to define a distribution ratio for sharing the energy fed by the two ESS. An overview of the closed-loop control of the multi-source EV is presented in Fig. 3.

For the DC bus inversion-based control, a reference current of the DC bus capacitor, i_{C_r} , is derived from a closed-loop control of the DC bus voltage, v_{DC} , by the inversion of (5):

$$i_{C_r} = (v_{DC_r} - v_{DC}) \cdot C_V(t) \quad (9)$$

where $C_V(t)$ is a voltage controller.

Thus, the reference for the total current, i'_{ESS_r} , is given by (10) and is obtained from the inversion of the upper equation of (6), using the measurement of the load current, i_t and the DC bus capacitor's reference current.

$$i'_{ESS_r} = i_t - i_{C_r} \quad (10)$$

On the DC bus side, the battery converter's current reference is obtained from i'_{ESS_r} and the inversion of the lower equation of (6) using a distribution ratio K_D , presented in (11).

$$i'^*_{bat_r} = K_D i'_{ESS_r}; \quad K_D \in [-1.5, 1.5] \quad (11)$$

To minimize stresses on the battery pack, two compensating elements are introduced in the establishment of the current reference: a low-pass filter (τ) and saturation limiters to prevent excessive discharge and charge currents based on the maximum battery current pack (I_{bat}^{max}). The resulting expression of saturation and low-pass filter usage in the reference current $i'^*_{bat_r}$ is given by:

$$i'^*_{bat_r} = \max\left(-\frac{1}{2} m_{bat} I_{bat}^{max}, \min\left(m_{bat} I_{bat}^{max}, \frac{i'^*_{bat_r}}{\tau \cdot s + 1}\right)\right) \quad (12)$$

Thus, the SCs current reference is computed using (13).

$$i'_{SC_r} = i_{t_r} - i'^*_{bat_r} \quad (13)$$

K_D defines the part of the total current that will be imposed to each source, and that will control the DC voltage. The strategy defined has to provide continuously changing values of K_D during the vehicle journey.

In order to obtain the reference current i_{j_r} , an inversion of (9) was used (14):

$$i_{j_r} = \frac{i'_{j_r}}{m_j} \quad (14)$$

A current controller is required to invert (7) and define the reference voltage $v_{ch_j_r}$ from i_{j_r} , using the v_j measurement as compensation for the controller, $C_{I_j}(t)$, defined by (15):

$$v_{ch_j_r} = v_j - (i_{j_r} - i_j) C_{I_j}(t) \quad (15)$$

For the EV speed inversion-based control, a controller, $C_S(t)$, is used to define the set point force, F_{tr_r} , from the EV speed reference, v_{EV_r} . This controller uses a rejection of the disturbance F_{env} and is provided by (16).

$$F_{tr_r} = (v_{EV_r} - v_{EV}) C_S(t) + F_{env} \quad (16)$$

The reference torque applied to the electrical motor, T_{em_r} , is deduced from the inversion of (4) given (17):

$$T_{em_r} = \frac{r}{G_{gb}} F_{tr_r} \quad (17)$$

B. Energy Management Strategy

The energy management problem consists in an on-line search of an optimal energy flow leading to the optimal use of the battery stored energy, while keeping SCs SoC within acceptable range. The energy management strategy needs to consider the available energy of both storage elements and instantaneously determines the power contribution between the two sources. The MCS described previously is able to receive references for different energy strategies. Using the macroscopic energy view for the studied EV (see Fig. 6), it is possible to understand the power flow between the different components and conveniently determine the membership function of the fuzzy logic controller [9].

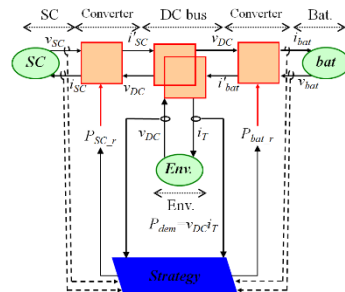


Fig. 6. High-level macroscopic energy view for the studied EV.

Fuzzy logic systems provide in a simple way to determine strategy laws using linguistic labels. This approach has been used in several other works to share the power demand in hybrid electric vehicles [9] and has been adopted to manage the hybrid ESS in this study. The global fuzzy logic system is presented in Fig. 7 (which is fully explained in [9]). The overall idea of the implemented energy strategy is that batteries will supply the propulsion power in steady state operations. For this reason, one input of the fuzzy logic controller is the ratio between the powers demanded by the powertrain P_{DC_bus} and the rated power that the batteries could provide to the DC bus. For an effective SCs operation, the energy strategy should regulate the SCs SoC. The second input of the fuzzy controller is the estimated value of SCs SoC.

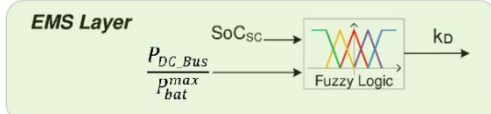


Fig. 7. Fuzzy logic strategy scheme.

The fuzzy controller therefore converts two clearly defined inputs into an output (16) using a normalized fuzzy logic strategy. Typically, fuzzy logic systems are designed from experience and the use of corresponding allows finding the membership function parameters. For evaluation purpose, the fuzzy membership function presented in [9], and validated by extended simulation processes, is illustrated in Fig. 8, and has been considered in (16):

$$K_D = f \left(SoC_{SCs}, \frac{P_{DC_Bus}}{P_{bat}^{max}} \right) \quad (16)$$

The fuzzy controller output (a relative change of K_D) is based on the rated limit of the battery pack power (P_{bat}^{max} , defined by the system designer according to the battery datasheet) and the SCs SoC. If the power ratio, P_{DC_Bus}/P_{bat}^{max} , is negative the powertrain operates in regenerative braking mode. In this situation, if the SCs SoC is lower than a defined threshold, K_D trends to zero, meaning that all the braking energy will be absorbed by the SCs. If the electric braking phase persists however, the SCs SoC may reach a higher level, close to a threshold value, inducing K_D to be raised to positive values in order to decrease the quantity of energy going to the SCs so as to prevent an “over voltage”.

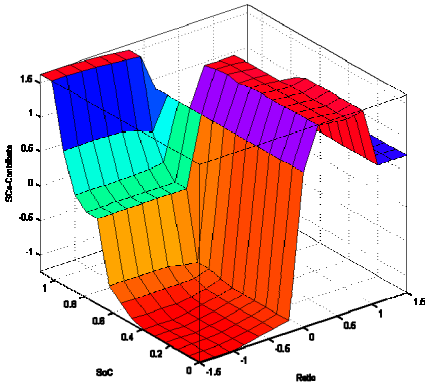


Fig. 8. Proposed output SCs contribution and its membership functions.

IV. SIMULATION RESULTS

The simulation was run in a Matlab/Simulink environment, using a PI controller for the current, voltage and powertrain. The driving cycles used for these tests were two concatenated driving cycles of NEDC ($t \in [0, 1800]$ s) and WMTC ($t \in [1200, 3000]$ s), and the initial SoC_{SCs} was 85% (considered “optimal” SoC level for the developed EMS [5]). The v_{DC} stability and the following current and speed references (Fig. 9-10), show the reliability of the controller. Analyzing the power demands from the batteries and SCs, the lower frequency of the battery currents can be seen when compared to the SCs currents. This result demonstrates that the strategy and decision making algorithm of the EMS is tuned.

Analyzing the results of Fig. 9-10, several general comments can be made. The batteries currents were kept below

its maximum level when discharging. Higher dynamic transitions were observed in the SCs in cases of higher power demanded by the powertrain. The EMS induces a behavior allowing the SCs SoC to return to its preset “optimal” value (85% in our case). During the deceleration phases, all the power flows to the SCs in order to recharge them, which demonstrates the importance of the “optimal” SoC level.

In Fig. 9, three different behavior of the SCs can be identified. During the first displacements of the vehicle, the batteries give the total power without the higher frequency transition (guaranteed by the SCs). For the displacement at higher speed, the batteries fed the system up to their maximum power while the SCs gave the rest. Finally, as the SoC is under the “optimal” level (due to the previous displacement), the EMS induce to SCs a controlled recharging process through the batteries in order to reach the “optimal” level.

Fig. 10 shows that the SCs voltage decreases to a minimum value near 1750 s, but the EMS allowed the SoC to be brought back to values up to 85%, without compromising the DC bus voltage stabilization. This means that the SCs SoC reaches acceptable values to give its contribution to the global feeding system. Near 1425 s, the highest power occurs demand where the contribution of each source is well balanced by the EMS.

V. CONCLUSIONS

A full-electric three-wheel roadster has been simulated using the EMR approach. The simulation results validate the proposed model based on EMR, the control layer and the proposed energy management strategy. This first step will be completed by introducing more accurate models to the proposed objectives of the studies and permits to take some decision in order to develop a deeper project under the battery/SCs hybridization for this kind of recreational vehicles. The coupling topology and hybridization, integrating a fuzzy logic controller EMS, was studied under simulation process for two major driving cycles. First simulation results depict a possible increase in the range autonomy coupled to smaller reduction in the batteries’ SoC at the end of the driving cycle. However, the hybrid ESS management problem is intrinsically linked to the ESS sizing and coupling them remains a crucial challenge.

Finally, this procedure is inserted into a more global approach in order to accelerate testing and validation time. The following steps will be based on extend the study with a reduced-scale prototype in a laboratory controlled environment before real-scale prototype implementation.

APPENDIX

Table III shows a summary of the EMR.

TABLE III. SUMMARY OF EMR PICTOGRAMS

	source element (energy source)		accumulation element (energy storage)		Indirect inversion (closed-loop control)		multi-physical conversion element
	mono-physical conversion element		mono-physical coupling element (energy distribution)		Direct inversion (open-loop control)		coupling inversion (energy criteria)

ACKNOWLEDGMENT

This work was supported in part by the Natural Sciences and Engineering Research Council of Canada.

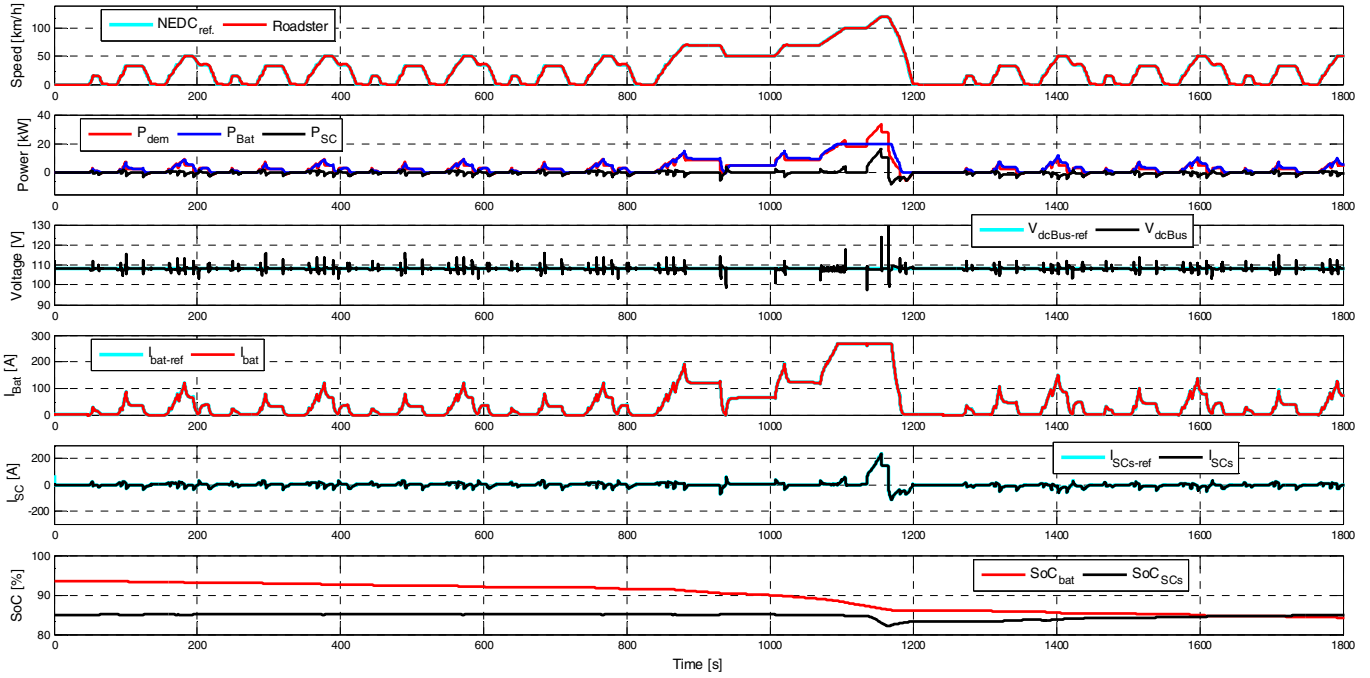


Fig. 9. Simulation results of the three-wheel roadster hybrid ESS for NEDC driving cycle.

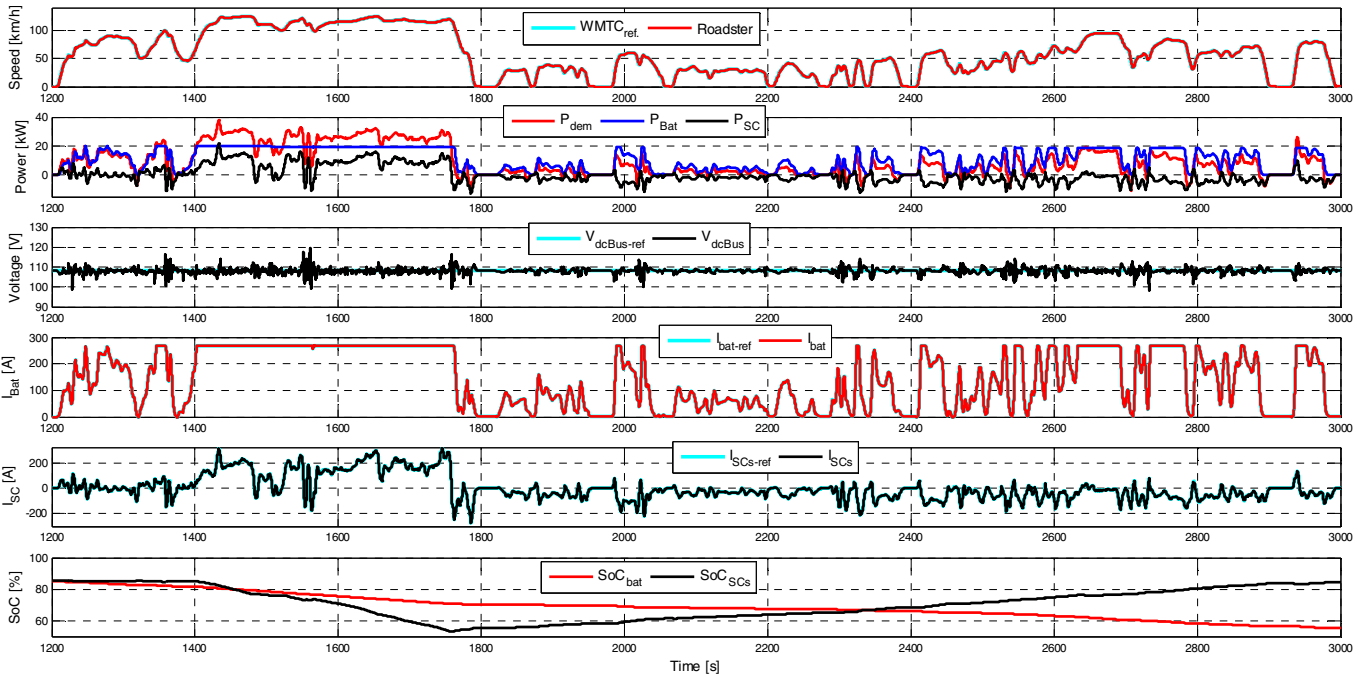


Fig. 10. Simulation results of the three-wheel roadster hybrid ESS for WMTC driving cycle.

REFERENCES

- [1] C.C. Chan, The state of the art of electric, hybrid, and fuel cell vehicles, *Proc. of the IEEE*, 95(4), pp. 704 – 718, April 2007.
- [2] R. Barrero, J. Van Mierlo, X. Tackoen, Energy savings in public transport, *IEEE Veh. Tec. Magazine*, 3 (3), pp. 26-36, Sep. 2008.
- [3] A. Khaligh, Z. Li, Battery, Ultracapacitor, Fuel Cell, and Hybrid Energy Storage Systems for Electric, Hybrid Electric, Fuel Cell, and Plug-In Hybrid Electric Vehicles: State of the Art, *IEEE Trans. Veh. Tec.*, 59 (6), pp. 2806-14, Jul. 2010.
- [4] T. Azib, O. Bethoux, G. Remy, C. Marchand, Saturation Management of a Controlled Fuel-Cell/Ultracapacitor Hybrid Vehicle, *IEEE Trans. Veh. Tec.*, 60 (9), pp. 4127-4138, Nov. 2011.
- [5] J. Trovão, P. G. Pereirinha, H. M. Jorge, C. H. Antunes, A multi-level energy management system for multi-source electric vehicles – An integrated rule-based meta-heuristic approach, *Applied Energy*, 105, pp. 304-318, May 2013.
- [6] A.-L. Allegre, A. Bouscayrol, R. Trigui, Flexible real-time control of a hybrid energy storage system for electric vehicles, *IET Electrical Systems in Transportation*, 3 (3), pp.79-85, Sep. 2013.
- [7] J. Trovão, A. Bouscayrol, F. Machado, W. Lhomme, Hierarchical Management Structure of a Battery Supercapacitor System for EV Using Energetic Macroscopic Representation, *11th International Conference on Modeling and Simulation of Electric Machines, Converters and Systems*, Valence, Spain, May 2014.
- [8] N. Denis, M. Dubois, R. Dubé, A. Desrochers, Blended Power Management Strategy Using Pattern Recognition for a Plug-in Hybrid Electric Vehicle, *Int. J. Intel. Transp. Syst. Res.*, Springer US, pp 1-14, Nov. 2014.
- [9] M. Silva, H. de Melo, J. P. Trovao, P. G. Pereirinha, H. M. Jorge, An Integrated Fuzzy Logic Energy Management for A Dual-Source Electric Vehicle, *39th Annual Conference of the IEEE Industrial Electronics Society (IECON 2013)*, pp.4564-4569, Nov. 2013.